IJE TRANSACTIONS A: Basics Vol. 26, No. 4, (April 2013) 421-432

International Journal of Engineering

Journal Homepage: www.ije.ir

RESEARCH NOTE

Elastoplastic Buckling Analysis of Plates Involving Free Edges by Deformation Theory of Plasticity

M. Maarefdoust*, M. Kadkhodayan

Department of Mechanical Engineering, Ferdowsi University of Mashhad, Mashhad, P.O. Box 91775-1111, Iran

PAPER INFO

Paper history:
Received 25 July 2012
Received in revised form 26 September 2012
Accepted 18 October 2012

Keywords:
Rectangular Plate
Deformation Theory
Loading Ratio
Elastoplastic Buckling
Aspects Ratio
GDQ

ABSTRACT

In this paper, elastoplastic buckling of rectangular plates with different boundary conditions is investigated. Differential governing equations of plate are obtained on the basis of general loading and according to deformation theory (DT) of plasticity. Various loading conditions such as uniaxial, biaxial and shear are studied. The employed material is AL7075T6 which is usually used in the aerospace industry. A wide range of aspect ratios and plate thicknesses are investigated. The generalized differential quadrature method (GDQ) is used as the numerical method to analysis the problem. The obtained results using deformation theory of plasticity are in good agreement with experimental data. An extensive parametric study for the effects of different aspects ratios, loading ratios, transverse shear deformations, thickness ratios and various boundary conditions on the buckling coefficient are presented.

doi: *10.5829/idosi.ije.2013.26.04a.11*

NOMENCLATURE

a	Length of plates [m]	$T(E_t)$	Tangent modulus [Pa]
b	Width of plates [m]	u, v, w	Displacement components
c, k	Ramberg-Osgood parameters	**Greek Symbols**	
D	Flexural rigidity of plates [N.m]	ϕ_x, ϕ_y	Rotations about x, y
E	Young's modulus of elasticity [Pa]	η	Thickness parameter
G	Effective shear modulus [Pa]	$\alpha, \beta, \gamma, \chi, \mu, \delta$	Parameters used in stress-strain relations
h	Thickness of plates [m]	κ^2	Shear correction factor
n	Number of node	ε_e	Total effective strain
K	Buckling coefficient	σ_e	Effective stress [Pa]
S_{ij}	Stress deviator tensor	υ	Poisson's ratio
$S(E_s)$	Secant modulus [Pa]	ξ	Loading ratio

1. INTRODUCTION

In the previous decades the problem of plastic buckling of plates was studied by many scientists. Indeed, the difference which exist in critical loads predicted by employing plasticity theories still is an open research issue. The first analysis of elasto-plastic buckling of plates was carried out by Anderson [1] using the energy stability criterion for rectangular plates under uniaxial compression. Shrivastava [2] studied on the plastic buckling of thick plates. The results showed that the decrease in plastic buckling stress parameters caused by the effect of transverse shear deformation was more in

*Corresponding Author Email: m_maarefdoost@yahoo.com (M. Maarefdoust)

incremental theory than deformation theory. But, this difference was not enough to fill the discrepancy between these two theories. Khdeir, et al. [3, 4] carried out the analysis of laminated plates with the use of first order and higher order deformation plate theories using Levy-type solution. But they were not able to apply the boundary conditions on a loaded free edge. Durban and Zuckerman [5] studied on the analysis of rectangular plates under uniaxial loading for several various modes with the separation of variables solution. However, the limited boundary conditions consisting of clamped and simply supported boundary conditions limited the obtained data in that research. Liew, et al. [6] solved the buckling plates with free edge for elastic mode and modified the Khdeir's boundary conditions. Durban [7] found out that the incremental theory can predict more buckling load in comparison with the deformation theory, and that the experimental data have more congruence with deformation theory. Of course, there are cases where the critical stresses obtained from two theories are nearly equal. A typical example is furnished by axially symmetric buckling of axially compressed circular cylindrical shells [8]. Chakrabarty, et al. [9] and Wang, et al. [10-12] investigated the elastic-plastic buckling of thin and thick plates based on deformation and incremental theories by use of separation of variables and Rayliegh-Ritz method. They came to the conclusion that the deformation theory predicts less buckling stress factor, and as the thickness and Ramberg-Osgood constant increases, the difference between two theories increases.

Since the free boundary conditions still have not received much attention in the literature, the authors have attempted in the current study to investigate the buckling problem of rectangular plates for various boundary conditions of FSFS, CSFS, SSFS using numerical method of GDQ and the results were compared with those available from previous studies.

2. GOVERNING DIFFERENTIAL EQUATIONS

The governing differential equations for elasto-plastic buckling of rectangular plates are mentioned elsewhere [12]. Figure 1 shows the sketch of a rectangular plate under biaxial and shear edge loads where a, b, h and ξ are the length, width, thickness of the plate and load ratio, respectively. The load ratio is ξ = 0 for uniaxial compression and ξ = 1 for the equibiaxial compression.

The relationship between the stress rate and strain rate in the plates are given below:

$$\begin{aligned}
\dot{\sigma}_x &= E\left(\alpha\dot{\varepsilon}_x + \beta\dot{\varepsilon}_y + \chi\dot{\gamma}_{xy}\right),\\
\dot{\sigma}_y &= E\left(\beta\dot{\varepsilon}_x + \gamma\dot{\varepsilon}_y + \mu\dot{\gamma}_{xy}\right),\\
\dot{\tau}_{xy} &= E\left(\chi\dot{\varepsilon}_x + \mu\dot{\varepsilon}_y + \delta\dot{\gamma}_{xy}\right),\\
\dot{\tau}_{xz} &= \kappa^2 G\dot{\gamma}_{xz},\ \dot{\tau}_{yz} = \kappa^2 G\dot{\gamma}_{yz},
\end{aligned} \tag{1}$$

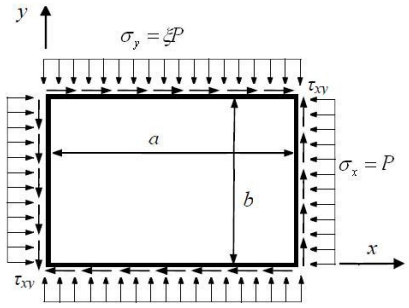

Figure 1. Sketch of a rectangular plate.

in which E, G and κ^2 are elastic modulus, effective shear modulus and shear correction factor, respectively. Parameters α, β, γ, χ, μ, δ and effective shear modulus depend on the plasticity theory employed. In the present study, the deformation theory of plasticity with Hencky constitutive equation is used. The fundamental equation of this theory is [9]:

$$E\dot{\varepsilon}_{ij} = \left(\frac{3E}{2S} - \frac{1-2\upsilon}{2}\right)\dot{S}_{ij} + \frac{1-2\upsilon}{3}\dot{\sigma}_{kk}\delta_{ij} + \frac{3\dot{\sigma}_e}{2\sigma_e}\left(\frac{E}{T} - \frac{E}{S}\right)S_{ij}, \tag{2}$$

where S is the secant modulus, T is the tangent modulus which is calculated through stress-strain curved and σe is the effective stress. The tangent modulus and effective stress are calculated as follow:

$$T = d\sigma_e / d\varepsilon_e, \quad \sigma_e^2 = \sigma_x^2 - \sigma_x\sigma_y + \sigma_y^2 + 3\tau_{xy}^2, \tag{3}$$

where ε_e is the total effective strain. The parameters α, β, γ, χ, μ, δ and shear modulus in this method are defined as follow [12]:

$$\begin{aligned}
&\alpha = \frac{1}{\rho}\left[c_{22}c_{33} - c_{23}^2\right], \beta = \frac{1}{\rho}\left[c_{13}c_{23} - c_{12}c_{33}\right],\\
&\gamma = \frac{1}{\rho}\left[c_{11}c_{33} - c_{13}^2\right], \mu = \frac{1}{\rho}\left[c_{12}c_{13} - c_{11}c_{23}\right],\\
&\chi = \frac{1}{\rho}\left[c_{12}c_{23} - c_{13}c_{22}\right], \delta = \frac{1}{\rho}\left[c_{11}c_{22} - c_{12}^2\right],\\
&\rho = \frac{E}{T}\begin{vmatrix} c_{11} & c_{12} & c_{13}\\ c_{21} & c_{22} & c_{23}\\ c_{31} & c_{32} & c_{33}\end{vmatrix}, \frac{E}{G_s} = 2 + 2\upsilon + 3\left(\frac{E}{S} - 1\right).
\end{aligned} \tag{4}$$

$$\begin{aligned}
c_{11} &= 1 - 3\left(1 - \frac{T}{S}\right)\left(\frac{\sigma_y^2}{4\sigma_e^2} + \frac{\tau_{xy}^2}{\sigma_e^2}\right),\\
c_{12} &= -\frac{1}{2}\left[1 - (1-2\upsilon)\frac{T}{E} - 3\left(1 - \frac{T}{S}\right)\left(\frac{\sigma_x\sigma_y}{2\sigma_e^2} + \frac{\tau_{xy}^2}{\sigma_e^2}\right)\right],\\
c_{13} &= \frac{3}{2}\left(1 - \frac{T}{S}\right)\left(\frac{2\sigma_x - \sigma_y}{\sigma_e}\right)\left(\frac{\tau_{xy}}{\sigma_e}\right),\\
c_{22} &= 1 - 3\left(1 - \frac{T}{S}\right)\left(\frac{\sigma_x^2}{4\sigma_e^2} + \frac{\tau_{xy}^2}{\sigma_e^2}\right),\\
c_{23} &= \frac{3}{2}\left(1 - \frac{T}{S}\right)\left(\frac{2\sigma_y - \sigma_x}{\sigma_e}\right)\left(\frac{\tau_{xy}}{\sigma_e}\right),\\
c_{33} &= 3\frac{T}{S} - (1-2\upsilon)\left(\frac{T}{E}\right) + 9\left(1 - \frac{T}{S}\right)\left(\frac{\tau_{xy}^2}{\sigma_e^2}\right).
\end{aligned} \tag{5}$$

The buckling equation of standard thick plates can be written as follow [9, 12]:

$$\kappa^2 G h\left(\frac{\partial \varphi_x}{\partial x}+\frac{\partial \varphi_y}{\partial y}+\nabla^2 w\right)=\sigma_x h\frac{\partial^2 w}{\partial x^2}+\sigma_y h\frac{\partial^2 w}{\partial y^2}+2\tau_{xy}h\frac{\partial^2 w}{\partial x\partial y}, \tag{6}$$

$$\frac{\partial}{\partial x}\left(\frac{\alpha Eh^3}{12}\frac{\partial \phi_x}{\partial x}+\frac{\beta Eh^3}{12}\frac{\partial \phi_y}{\partial y}+\frac{\chi Eh^3}{12}\left(\frac{\partial \phi_x}{\partial y}+\frac{\partial \phi_y}{\partial x}\right)\right)+\frac{\partial}{\partial y}\left[\frac{\delta Eh^3}{12}\left(\frac{\partial \phi_x}{\partial y}+\frac{\partial \phi_y}{\partial x}\right)+\frac{\chi Eh^3}{12}\frac{\partial \phi_x}{\partial x}+\frac{\mu Eh^3}{12}\frac{\partial \phi_y}{\partial y}\right]-\kappa^2 Gh\left(\phi_x+\frac{\partial w}{\partial x}\right)=0, \tag{7}$$

$$\frac{\partial}{\partial y}\left(\frac{\gamma Eh^3}{12}\frac{\partial \phi_y}{\partial y}+\frac{\beta Eh^3}{12}\frac{\partial \phi_x}{\partial x}+\frac{\mu Eh^3}{12}\left(\frac{\partial \phi_x}{\partial y}+\frac{\partial \phi_y}{\partial x}\right)\right)+\frac{\partial}{\partial x}\left[\frac{\delta Eh^3}{12}\left(\frac{\partial \phi_x}{\partial y}+\frac{\partial \phi_y}{\partial x}\right)+\frac{\chi Eh^3}{12}\frac{\partial \phi_x}{\partial x}+\frac{\mu Eh^3}{12}\frac{\partial \phi_y}{\partial y}\right]-\kappa^2 Gh\left(\phi_y+\frac{\partial w}{\partial y}\right)=0. \tag{8}$$

Note that Equations (4)-(8) are re-derived and extended and are slightly different from the ones given in other references [9].

3. GOVERNING BOUNDARY CONDITIONS

The boundary conditions are [9]:

$$\begin{aligned} &W=0,\ \phi_y=0,\ M_{xx}=0, \qquad for\ \ x=0,\ x=a\\ &W=0,\ \phi_x=0,\ M_{yy}=0, \qquad for\ \ y=0,\ y=b\end{aligned} \tag{9}$$

for simply support edges and

$$W=0,\ \phi_x=0,\ \phi_y=0, \qquad for\ \ x=0,\ x=a \tag{10}$$

for clamped edges. For free boundary conditions we have [12]:

$$M_{xx}=0,\ M_{yx}=0,\ Q_x=0, \quad for\ \ x=0,\ x=a \tag{11}$$

where,

$$\begin{aligned} M_{xx}&=\frac{Eh^3}{12}\left(\alpha\frac{\partial \phi_x}{\partial x}+\beta\frac{\partial \phi_y}{\partial y}\right),\\ M_{yy}&=\frac{Eh^3}{12}\left(\beta\frac{\partial \phi_x}{\partial x}+\gamma\frac{\partial \phi_y}{\partial y}\right),\\ M_{xy}&=M_{yx}=\frac{Gh^3}{12}\left(\frac{\partial \phi_x}{\partial y}+\frac{\partial \phi_y}{\partial x}\right),\\ Q_x&=\kappa^2 Gh\left(\phi_x+\frac{\partial w}{\partial x}\right)-\sigma_x h\frac{\partial w}{\partial x},\\ Q_y&=\kappa^2 Gh\left(\phi_y+\frac{\partial w}{\partial y}\right)-\sigma_y h\frac{\partial w}{\partial y}.\end{aligned} \tag{12}$$

In the present study, in addition to re-investigation of SSSS mode, the other modes including CSFS, SSFS and FSFS are investigated.

4. GENERALIZED DIFFERENTIAL QUADRATURE METHOD

This method (GDQ) is a practical and simple in solving engineering problem. It was in 1971 that Belman, et al. [13] introduced the ordinary or partial equation as a new technique for numerical solving. Their purpose was to present a new way for overcoming the constant problems and amount of numerical problems. The first widespread use of this technique in the field of engineering problems was given by Bert and Malik [14].

The benefit of accessing to a new and exact solution with the least analysis in comparison to others numerical solutions like finite element and boundary element causes the efficiency of this method to be revealed gradually. This method can solve higher order differential equations with selecting few grid spacing. The essence of the GDQ method is that the partial derivative of a function with respect to a variable is approximated by a weighted sum of function values at all discrete points in that direction. Its weighting coefficients do not relate to any special problem and only depend on the grid spacing. Thus, any partial differential equation can be easily reduced to a set of algebraic equations using these coefficients.

Its other characteristics are simple application, programming and high convergence rate. The distributions of grid spacing of Chebyshev–Guass–Lobatto have the best convergence and highest accuracy [15, 16]. In this study, the following relation is used:

$$x_i=\frac{1}{2}(1-Cos\frac{i-1}{n-1}\pi)\ ,\ i=1,2,.....,n \tag{13}$$

With the aid of GDQ, the governing Equations (6)-(8) can be shown as follow:

$$\kappa^2 Gh\Big(\sum_{m=1}^{N_x}A_{im}^x\phi_{mj}^x+\sum_{n=1}^{N_y}A_{jn}^y\phi_{in}^y+\sum_{m=1}^{N_x}B_{im}^x W_{mj}+\sum_{n=1}^{N_y}B_{jn}^y W_{in}\Big)=\sigma_x h\sum_{m=1}^{N_x}B_{im}^x W_{mj}+\sigma_y h\sum_{n=1}^{N_y}B_{jn}^y W_{in}+2\tau_{xy}h\sum_{m=1}^{N_x}\sum_{n=1}^{N_y}A_{im}^x A_{jn}^y W_{mn}, \tag{14}$$

$$\frac{\alpha Eh^3}{12}\sum_{m=1}^{N_x}B_{im}^x\phi_{mj}^x+\frac{\beta Eh^3}{12}\sum_{m=1}^{N_x}\sum_{n=1}^{N_y}A_{im}^x A_{jn}^y\phi_{mn}^y+\frac{\chi Eh^3}{12}\left(\sum_{m=1}^{N_x}\sum_{n=1}^{N_y}A_{im}^x A_{jn}^y\phi_{mn}^x+\sum_{m=1}^{N_x}B_{im}^x\phi_{mj}^y\right)+\frac{\delta Eh^3}{12}\left(\sum_{n=1}^{N_y}B_{jn}^y\phi_{in}^x+\sum_{m=1}^{N_x}\sum_{n=1}^{N_y}A_{im}^x A_{jn}^y\phi_{mn}^x\right)+\frac{\chi Eh^3}{12}\sum_{m=1}^{N_x}\sum_{n=1}^{N_y}A_{im}^x A_{jn}^y\phi_{mn}^x+\frac{\mu Eh^3}{12}\sum_{n=1}^{N_y}B_{jn}^y\phi_{in}^y-\kappa^2 Gh\left(\phi_{ij}^x+\sum_{m=1}^{N_x}A_{im}^x W_{mj}\right)=0, \tag{15}$$

$$\frac{\gamma Eh^3}{12}\sum_{m=1}^{N_x} B_{jn}^{y}\phi_{in}^{y} + \frac{\beta Eh^3}{12}\sum_{m=1}^{N_x}\sum_{n=1}^{N_y} A_{im}^{x}A_{jn}^{y}\phi_{mn}^{x} +$$
$$\frac{\mu Eh^3}{12}\left(\sum_{m=1}^{N_x}\sum_{n=1}^{N_y} A_{im}^{x}A_{jn}^{y}\phi_{mn}^{y} + \sum_{n=1}^{N_y} B_{jn}^{x}\phi_{in}^{x}\right) +$$
$$\frac{\delta Eh^3}{12}\left(\sum_{m=1}^{N_x}\sum_{n=1}^{N_y} A_{im}^{x}A_{jn}^{y}\phi_{mn}^{x} + \sum_{m=1}^{N_x} B_{im}^{x}\phi_{mj}^{y}\right) + \quad (16)$$
$$\frac{\chi Eh^3}{12}\left(\sum_{m=1}^{N_x} B_{im}^{x}\phi_{mj}^{x}\right) + \frac{\mu Eh^3}{12}\sum_{m=1}^{N_x}\sum_{n=1}^{N_y} A_{im}^{x}A_{jn}^{y}\phi_{mn}^{y}$$
$$-\kappa^2 Gh\left(\phi_{ij}^{y} + \sum_{n=1}^{N_y} A_{jn}^{y}W_{in}\right) = 0,$$

where A and B are the first and the second order derivatives, respectively. Now, the buckling coefficient K can be defined as:

$$K = \frac{\sigma_c hb^2}{\pi^2 D} = \frac{\sigma_c(1-\upsilon^2)b^2}{E\eta a^2}, \quad (17)$$

where D is the flexural rigidity and η is the thickness parameter as follows:

$$D = \frac{Eh^3}{12(1-\nu^2)}, \qquad \eta = \frac{\pi^2 h^2}{12\,a^2}. \quad (18)$$

5. RESULTS AND DISCUSSIONS

The material used in this study is AL 7075-T6. Here the Ramberg-Osgood elasto-plastic stress-strain relationship is used:

$$\varepsilon = \frac{\sigma_e}{E} + \frac{k\sigma_0}{E}\left(\frac{\sigma_e}{\sigma_0}\right)^c, \quad (19)$$

where ε is the total plastic strain and c and k are material parameters. The tangent and secant moduli used in the equation are calculated as follow:

$$\frac{E}{T} = 1 + ck\left(\frac{\sigma_e}{\sigma_0}\right)^{c-1}, (c \succ 1)$$
$$\frac{E}{S} = 1 + k\left(\frac{\sigma_e}{\sigma_0}\right)^{c-1}, (c \succ 1). \quad (20)$$

The characteristics of this metal is obtained by means of Equation (19), $E/\sigma_0 = 150$, Ramberg-Osgood parameters c = 9.2 and k = 3/7, shear correction factor $\kappa^2 = 5/6$ and Poisson's ratio ν = 0.33 [12]. Figure 2 shows the Ramberg-Osgood stress–strain relation for the material AL 7075-T6 described by Equation (19). To increase the accuracy of the analysis, the grid spacing and mesh sensitivity have to be selected properly. As shown in Figure 3, the numbers of grid points are 13. It is seen that the convergence rate of GDQ method is excellent.

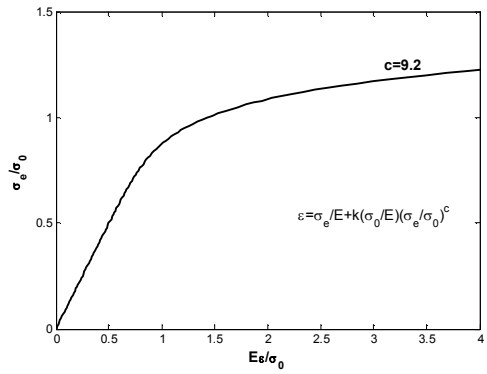

Figure 2. Ramberg-Osgood stress–strain relation for AL 7075-T6.

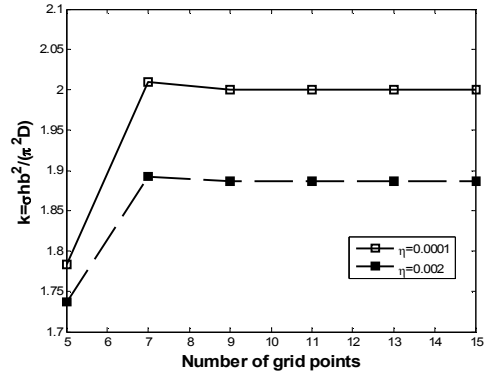

Figure 3. Mesh sensitivity curve for SSSS plate.

To verify the current study, some of the obtained results are firstly compared with some reference [3] and then some new results are presented. The buckling coefficient (K) in terms of loading ratio (ξ) for different thickness parameters (η) were calculated by deformation theory for SSSS plate, and it is observed that there is a good consistency between the current results and some reference [5] for rectangular plate of a/b = 1, Figure 4. In this case, the square plate under biaxial compression, buckling occurs in elastic mode when η = 0.0001 and the obtained results from deformation theory are in agreement with some reference [5]. Moreover, to check the accuracy of the obtained results, they are compared with some previous results, see Table 1.

A comparison between the obtained results and experimental data for rectangular plates under uniaxial compression are presented in Figure 5. It can be seen that the results attained by deformation theory are close to the experimental ones.

5. 1. Effect of Aspect Ratio on the Critical Buckling Load Figure 6 shows the relationship between the buckling coefficient and plate aspect ratio

TABLE 1. Comparison between the buckling coefficient for plates under uniaxial and equibiaxial loads with different thickness parameters.

BC		$\eta = 0.0001$	$\eta = 0.002$	$\eta = 0.008$
SSSS (uniaxial)	Durban et al.,[5]	4.0000	-----	-----
	Wang et al., [9]	4.0000	2.7954	0.9144
	Wang et al., [12]	4.0000	2.7954	0.9144
	Shrivastava [2]	4.0000	2.8058	0.9205
	Present study(GDQ)	**4.0000**	**2.7954**	**0.9144**
FSFS (Equibiaxial)	Wang et al., [9]	0.9158	0.9032	0.6250
	Wang et al., [12]	0.9159	0.9033	0.6249
	Present study(GDQ)	**0.9159**	**0.9032**	**0.6249**

for FSFS rectangular plates for various thickness ratios (h/b) in three modes including axial compression (ξ=0), biaxial compression (ξ=1) and shear obtained by deformation theory. In FSFS thin plates (h/b ≤ 0.05), the buckling coefficient in uniaxial compression increases as the plate aspect ratio increases in a range of 0.5≤ a/b ≤1.3.

When the aspect ratio increases further, the buckling mode shape switches from asymmetric to symmetric and then no more mode change is observed by increasing the aspect ratio (Figure 7). However, for higher thickness ratios (h/b), the variation of aspect ratio has not significant influence on the buckling coefficient (Figure 6a). In equibiaxial compression, the buckling coefficient increases monotonically and with increasing the aspect ratio no mode shape shift is observed (Figures 6b and 8b-8c).

In thin plates (h/b≤0.05) the changes of buckling mode shape is more obvious than that of the thick plates (0.05≤h/b) when buckling occurs in plastic mode [9]. Figure 6 also provides some information about the effect of transverse shear deformation on the buckling coefficients which decreases as the plate thickness ratio (h/b) increases.

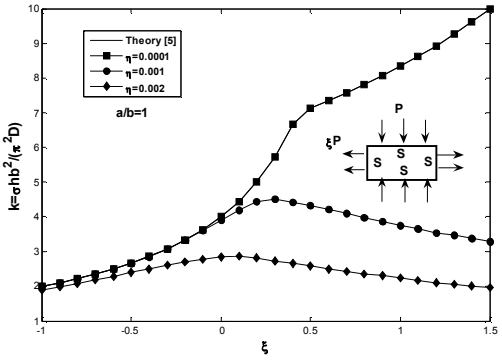

Figure 4. Comparison of deformation theory with Durban solutions for SSSS square plate for different thickness parameteres.

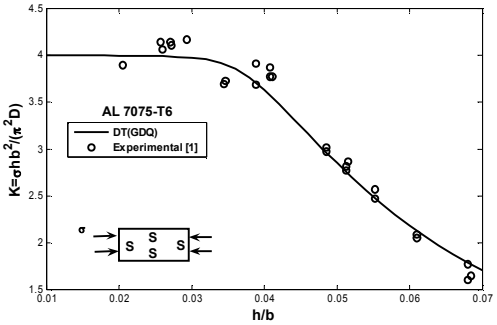

Figure 5. Comparison of buckling coefficient obtained by deformation theory with experimental data for SSSS square plate under uniaxial compression.

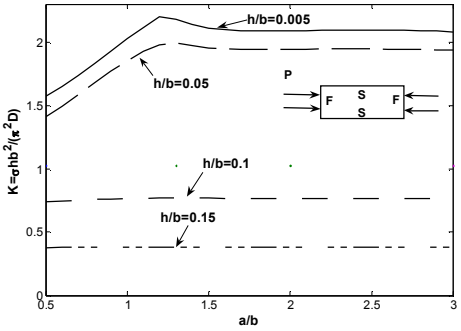

(a)

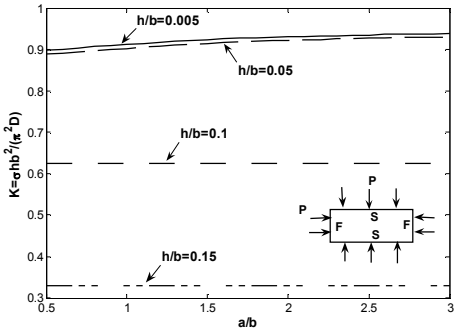

(b)

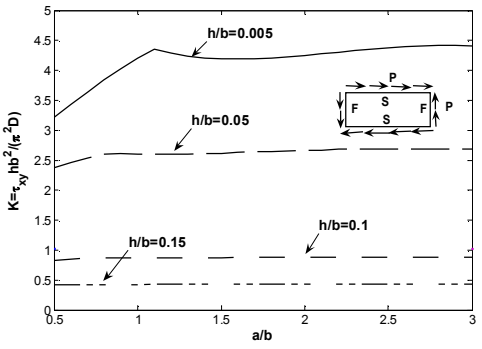

(c)

Figure 6. Variation of buckling coefficient with aspect ratio for different thickness ratios (h/b) based on deformation theory for various loading in FSFS plate.

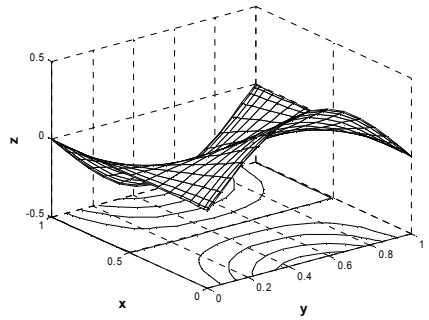

(a)

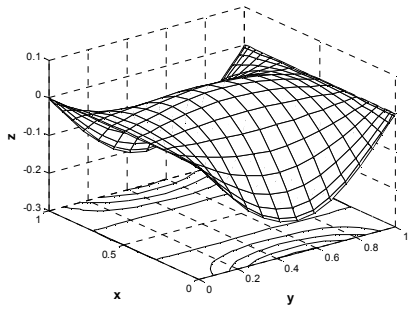

(b)

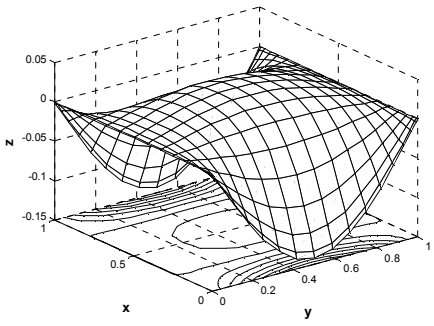

(c)

Figure 7. The critical buckling mode shape for FSFS plate under uniaxial loading in various aspect ratios for h/b= 0.005, (a) a/b=0.5; (b) a/b=1.3 and (c) a/b=2.2.

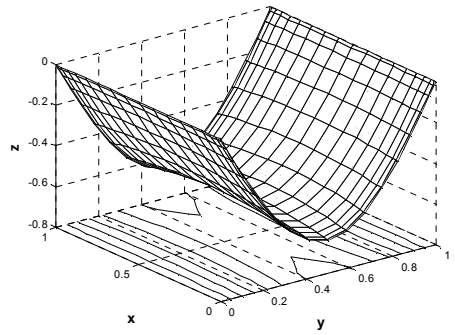

(a)

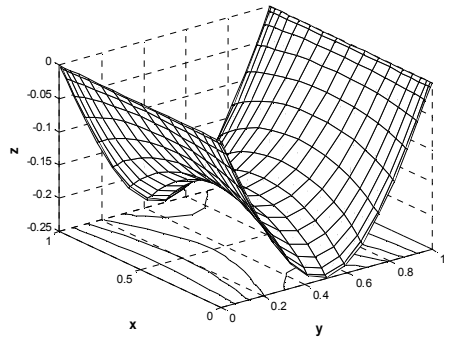

(b)

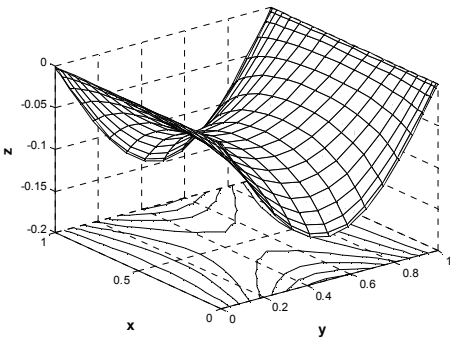

(c)

Figure 8. The critical buckling mode shape for FSFS plate under equibiaxial loading in various aspect ratios for h/b= 0.005, (a) a/b= 0.5; (b) a/b= 1.3 and (c) a/b= 2.2 .

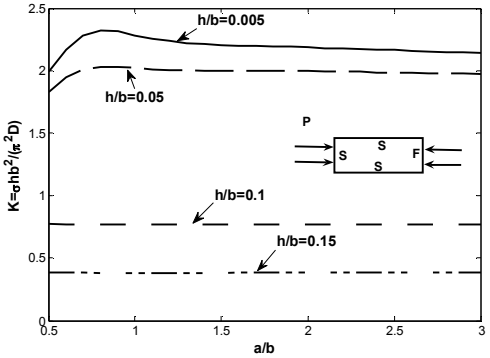

(a)

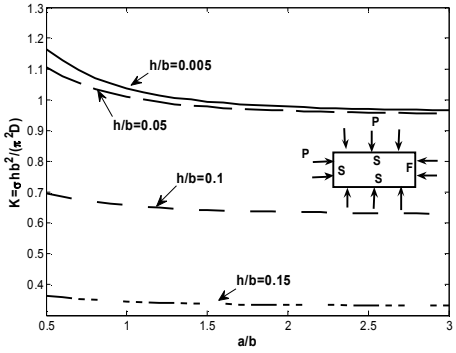

(b)

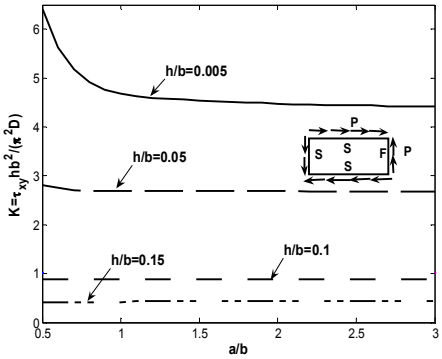

(c)

Figure 9. Variation of buckling coefficient with aspect ratio for different thickness ratios (h/b) based on deformation theory in various loadings for SSFS plate.

In SSFS thin plate, the buckling coefficient in uniaxial compression increases as the aspect ratio increases up to 0.75 and then decreases (Figure 9a). The limitations of aspect ratio ($0.5 \leq a/b \leq 0.75$) to increase the buckling coefficient is smaller than those of the previous mode ($0.5 \leq a/b \leq 1.2$). Moreover, with increasing the thickness, the changes of aspect ratio is not significant on buckling coefficient (Figure 9a).

Buckling mode deformation occurs in ($a/b = 0.75$). In equibiaxial compression mode, however, the buckling coefficient steadily decreases as the aspect ratio increases and no mode shape shift is observed (Figure 9b).

In shear mode, with increasing the aspect ratio the buckling coefficient decreases and with increasing the thickness of plate, the changes of aspect ratio has no influence on the buckling coefficient (Figure 9c).

In CSFS plate, and in uniaxial compression, with increasing the aspect ratio, the buckling coefficient decreases. There are mode shape shifts in this case again although the shift points are not so clear (Figure 10a). However, in equibiaxial compression and shear loading, the buckling coefficient decreases monotonically as the aspect ratio changes from 0.5 to 3 and no mode shape shift is evident in this case (Figures 10b-10c).

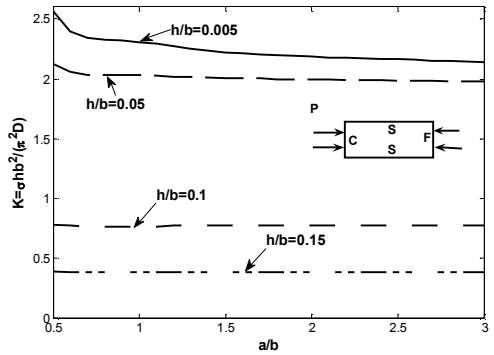

(a)

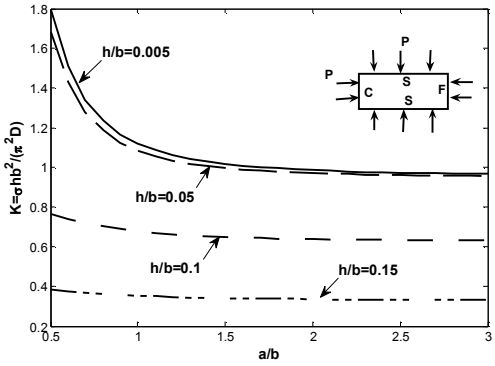

(b)

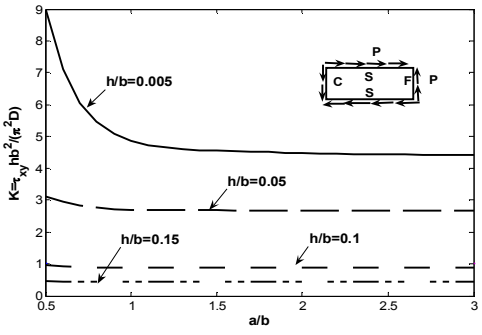

(c)

Figure 10. Variation of buckling coefficient with aspect ratio for different thickness ratios (h/b) based on deformation theory in different loading conditions for CSFS plate.

With increasing the aspect ratio, the reduction of buckling coefficient in CSFS is more than that of SSFS for different loading cases (Figures 9 and 10). In contrast to the CSFS plate subjected to uniaxial compression which shows decreasing of buckling coefficient with increase of aspect ratio, for FSFS and SSFS plates firstly an initial increase and then a steadily decrease is observed (Figures 6a, 9a and 10a). For the equibiaxial compression, however, the buckling coefficient increases for higher aspect ratios in FSFS plate which is different from CSFS and SSFS cases (Figures 6b, 9b and 10b).

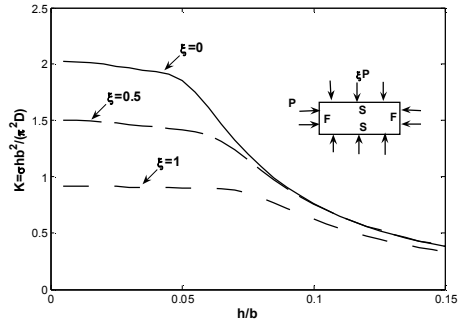

(a)

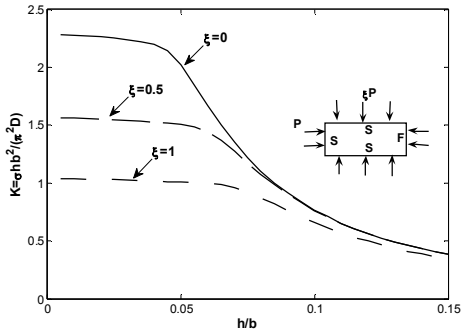

(b)

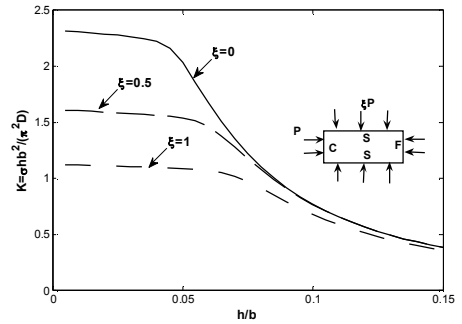

(c)

Figure 11. Variation of buckling coefficient with plate thickness ratio for different loading ratios based on deformation theory.

From Figures 9a and 10a, it can be clearly seen that in uniaxial compression mode with the increase of aspect ratio (a/b≥2), the change of boundary conditions from simply support (x = 0) to clamp doesn't have any significant effect on the results of buckling coefficient. Moreover, the effect of transverse shear deformation can also be seen here in Figures 9 and 10.

5. 2. Effect of Loading Ratio on the Critical Buckling Load The effect of loading ratio on the buckling coefficient for rectangular plates with the boundary conditions of FSFS, SSFS and CSFS are shown in Figure 11. It is seen that with increase of loading ratio in all three cases, the buckling coefficients decrease. Moreover, with increasing the thickness ratio the buckling coefficients for different loading ratios ($\xi \geq 0$) approach to each other (Figure 11). Furthermore, the buckling coefficients decrease as the thickness ratios increase for all cases.

Similarly, it is seen that the effect of transverse shear deformation on the buckling coefficient is more pronounced in plates subjected to uniaxial compression (ξ=0) than that in biaxial compression (ξ=0.5 and 1.0), Figures 11a-11c. This effect is marginally greater in the CSFS plate than those in SSFS and FSFS plates.

5. 3. Effect of Thickness Ratio on the Critical Buckling Load Figure 12 shows that with increasing the loading ratio, buckling coefficient decreases. This reduction occurs more rapidly for thinner plates. In FSFS plate, the mode deformation occurs in the range of $0.6 \leq \xi \leq 0.72$ for plates with different thicknesses (Figure 12a). The rate of reduction in the buckling coefficient accelerates when the load ratio reaches these mode shape shift points.

The buckling mode shapes for different boundary conditions under uniaxial and equibiaxial loadings for (a) FSFS, (b) SSFS and (c) CSFS plates are demonstrated in Figures 13 and 14. It is observed that for a/b = 1 and h/b = 0.005, the SSFS and CSFS square plates under uniaxial and equibiaxial loadings buckle in higher mode shape, but the FSFS square plate buckles in the first mode shape, Figures (13a-13c, 6a, 9a and 10a).

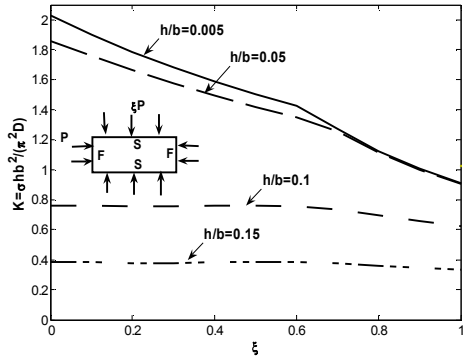

(a)

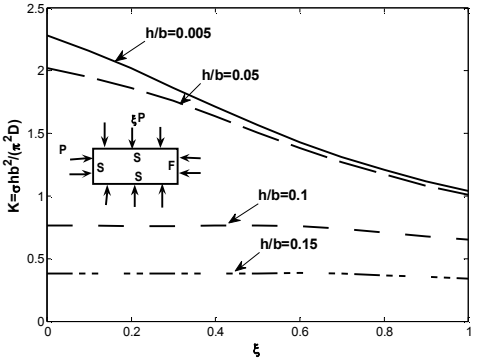

(b)

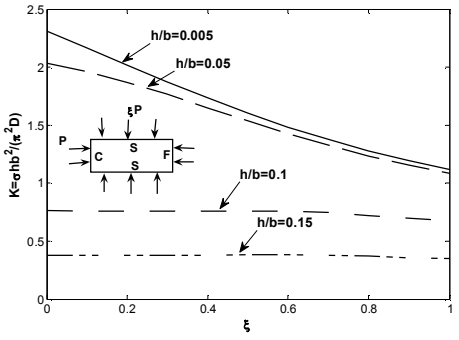

(c)

Figure 12. Variation of buckling coefficient with loading ratios for different plate thickness ratios based on deformation theory.

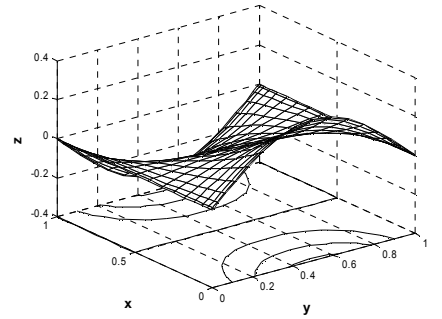

(a)

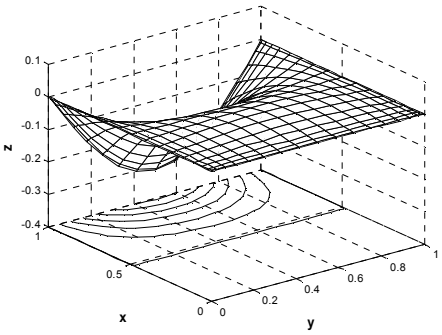

(b)

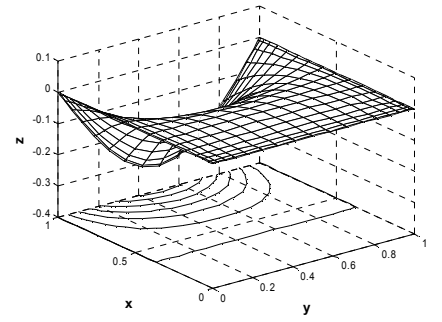

(c)

Figure 13. The critical buckling mode shapes for different boundary conditions under uniaxial loading (a) FSFS; (b) SSFS and (c) CSFS plates (h/b = 0.005, a/b=1).

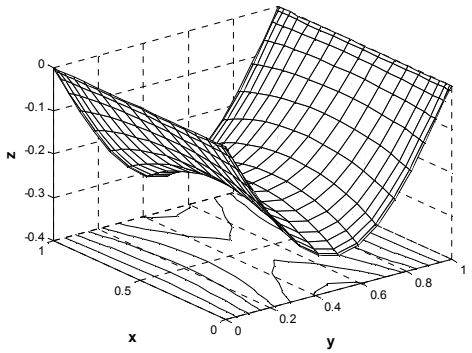

(a)

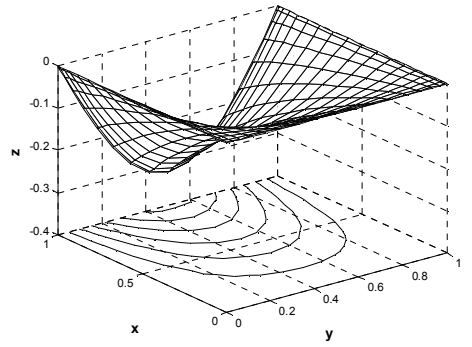

(b)

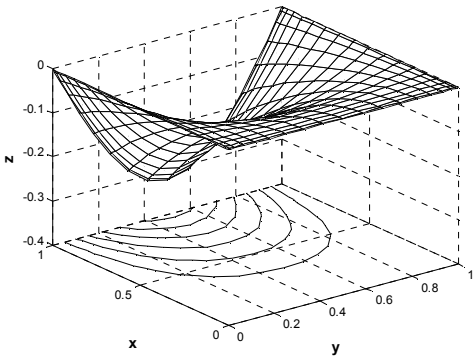

(c)

Figure 14. The buckling mode shapes for different boundary conditions under equibiaxial loading (a) FSFS; (b) SSFS and (c) CSF S plates (h/b = 0.005, a/b = 1).

6. CONCLUSION

The elasto-plastic buckling of rectangular plates with the use of deformation theory of plates was investigated. The equilibrium equations of the thick plate were derived by the aid of Hencky constitutive equations. The generalized differential quadrature method was employed to solve the governing differential equations. Some of the obtained results were compared with the previous reported data in the literature and some other results were presented. It was found that the results

obtained from deformation theory of plates formulation are in good agreement with those of experimental data.

The effect of boundary condition, transverse shear deformation, loading conditions, aspect ratio, and thickness and loading ratio on the buckling coefficient were investigated and discussed in detail and the buckled mode shapes could be easily plotted. Based on the numerical results, some more important conclusions are highlighted as follow:

- In the same boundary conditions, the maximum and minimum buckling coefficients occurred in equibiaxial and shear loadings, respectively.
- In various loadings and boundary conditions, most variations of buckling coefficient occurred in the range of $0.5 \leq a/b \leq 1.0$.
- In thick plates ($0.05 \leq h/b \leq 0.1$), with increasing the thickness in various boundary conditions the variation of aspect ratio had not significant influence on the buckling coefficient in uniaxial and shear loadings. However, for the case of equibiaxial loading some slight effects could be observed.
- In various boundary conditions and in equibiaxial loading, with increasing the loading ratio ($0 \leq \xi \leq 1.0$) the buckling coefficient decreased.
- In different loading ratios ($0 \leq \xi \leq 1.0$), the variation ranges of buckling coefficients in thin plates were much more than those in thick plates.
- The effects of transverse shear deformations on the buckling coefficients were more dominant in uniaxial compression than that in the biaxial compression plates.

7. REFERENCES

1. Anderson, R. A. and Anderson, M. S., Correlation of crippling strength of plate structures with material properties., NACA Technical Note 3600: Washington, D.C., (1956), 1-50.
2. Shrivastava, S., "Inelastic buckling of plates including shear effects", ***International Journal of Solids and Structures***, Vol. 15, No. 7, (1979), 567-575.
3. Khdeir, A. and Librescu, L., "Analysis of symmetric cross-ply laminated elastic plates using a higher-order theory: Part ii—buckling and free vibration", ***Composite Structures***, Vol. 9, No. 4, (1988), 259-277.
4. Khdeir, A., "Free vibration and buckling of symmetric cross-ply laminated plates by an exact method", ***Journal of Sound and Vibration***, Vol. 126, No. 3, (1988), 447-461.
5. Durban, D. and Zuckerman, Z., "Elastoplastic buckling of rectangular plates in biaxial compression/tension", ***International Journal of Mechanical Sciences***, Vol. 41, No. 7, (1999), 751-765.
6. Liew, K., Xiang, Y. and Kitipornchai, S., "Analytical buckling solutions for mindlin plates involving free edges", ***International Journal of Mechanical Sciences***, Vol. 38, No. 10, (1996), 1127-1138.
7. Durban, D., "Plastic buckling of plates and shells", ***Stability Analysis of Plates and Shells: a Collection of Papers in Honor of Dr. Manuel Stein***, ID. 206280, (1998), 293-301.
8. Ore, E. and Durban, D., "Elastoplastic buckling of axially compressed circular cylindrical shells", ***International Journal of Mechanical Sciences***, Vol. 34, No. 9, (1992), 727-742.
9. Wang, C., Xiang, Y. and Chakrabarty, J., "Elastic/plastic buckling of thick plates", ***International Journal of Solids and Structures***, Vol. 38, No. 48, (2001), 8617-8640.
10. Wang, X. and Huang, J., "Elastoplastic buckling analyses of rectangular plates under biaxial loadings by the differential qudrature method", ***Thin-Walled Structures***, Vol. 47, No. 1, (2009), 14-20.
11. Chakrabarty, J., "Applied plasticity", Springer, (2009).
12. Wang, C. and Aung, T. M., "Plastic buckling analysis of thick plates using p-ritz method", ***International Journal of Solids and Structures***, Vol. 44, No. 18, (2007), 6239-6255.
13. Bellman, R. and Casti, J., "Differential quadrature and long-term integration", University of Southern California, Los Angeles (USA); RAND Corp., Santa Monica, CA (USA). (1970).
14. Bert, C. W. and Malik, M., "Differential quadrature method in computational mechanics: A review", ***Applied Mechanics Reviews***, Vol. 49, No., (1996), 1-27.
15. Shu, C., Chen, W., Xue, H. and Du, H., "Numerical study of grid distribution effect on accuracy of DQ analysis of beams and plates by error estimation of derivative approximation", ***International Journal for Numerical Methods in Engineering***, Vol. 51, No. 2, (2001), 159-179.
16. Shu, C. and Richard, B., "Parallel simulation of incompressible viscous flows by generalized differential quadrature", ***Computing Systems in Engineering***, Vol. 3, No. 1, (1992), 271-281.

Elastoplastic Buckling Analysis of Plates Involving Free Edges by Deformation Theory of Plasticity

RESEARCH NOTE

M. Maarefdoust, M. Kadkhodayan

Department of Mechanical Engineering, Ferdowsi University of Mashhad, Mashhad, P.O. Box 91775-1111, Iran

P A P E R I N F O

Paper history:
Received 25 July 2012
Received in revised form 26 September 2012
Accepted 18 October 2012

Keywords:
Rectangular Plate
Deformation Theory
Loading Ratio
Elastoplastic Buckling
Aspects Ratio
GDQ

چکیده

در این مقاله کمانش الاستوپلاستیک صفحات مستطیلی با شرایط مرزی مختلف مورد بررسی قرار می‌گیرد. معادلات دیفرانسیل حاکم بر صفحه در حالات بارگذاری کلی و بر اساس تئوری پلاستیسیته تغییرشکل (DT) استخراج گردیده است. بارگذاری‌های مختلفی شامل تک محوری، دو محوری و برشی مطالعه می‌شود. ماده مورد استفاده آلومینیوم (7075T6) است که معمولا در صنعت هوافضا مورد استفاده قرار می‌گیرد. محدودهٔ وسیعی از نسبت طول به عرض و ضخامت صفحه مطالعه می‌شود. روش یک چهارم تفاضلی تعمیم یافته به عنوان روش عددی برای تحلیل مساله مورد استفاده قرار می‌گیرد. مقایسه نتایج عددی با نتایج آزمایشگاهی نشان از دقت خوب تئوری تغییرشکل در محاسبه ضریب کمانش الاستوپلاستیک صفحات دارد. مطالعهٔ پارامتریک وسیعی در مورد اثر نسبت ابعادی، ضریب بار، تغییرشکل برشی عرضی، ضریب ضخامت و شرایط مرزی مختلف بر ضریب کمانش انجام گرفته است .

doi: *10.5829/idosi.ije.2013.26.04a.11*